NMDA receptor hypofunction phase-couples independent gamma oscillations in the rat visual cortex.

Himashi Anver, Peter D Ward, Andor Magony, Martin Vreugdenhil

Title:

NMDA receptor hypofunction phase-couples independent gamma oscillations in the rat visual cortex.

Authors:

Himashi Anver, Peter D. Ward, Andor Magony and Martin Vreugdenhil (PhD)

Institution:

Neuronal Networks Group, School of Clinical and Experimental Medicine, University of Birmingham, Birmingham, B15 2TT, United Kingdom

Correspondence to:

Dr. M. Vreugdenhil, Neuronal Networks Group, School of Clinical and Experimental Medicine, University of Birmingham, B15 2TT, Birmingham, United Kingdom. Phone: +44 121 4147629; Fax: +44 121 4147625; Email: m.vreugdenhil@bham.ac.uk

Running title:

Hallucinogenic gamma oscillation phase-coupling

Abstract

Hallucinations, a hallmark of psychosis, can be induced by the psychotomimetic NMDA receptor antagonists ketamine and phencyclidine and are associated with hypersynchronization in the gamma frequency band, but it is unknown how reduced interneuron activation, associated with NMDA receptor hypofunction can cause hypersynchronisation or distorted perception. Low-frequency gamma oscillations (LFγ) and high-frequency gamma oscillations (HFγ) serve different aspects of perception. Here we test whether ketamine and phencyclidine are able to affect the interactions between HFγ and LFγ in the rat visual cortex *in vitro*.

In slices of the rat visual cortex kainate and carbachol induced LFγ (~34 Hz at 32 ºC) in layer V and HFγ (~54 Hz) in layer III of the same cortical column. In control HFγ and LFγ were independent and pyramidal neurons recorded in layer III were entrained by HFγ, but not by LFγ. Sub-anaesthetic concentrations of ketamine selectively decelerated HFγ by 22 Hz (EC_{50}= 2.7 μM), to match the frequency of LFγ in layer V. This caused phase-coupling of the two gamma oscillations, increased spatial coherence in layer III and entrained the firing of layer III pyramidal neurons by LFγ in layer V. Phencyclidine similarly decelerated HFγ by 22 Hz (EC_{50}= 0.16 μM), causing cross-layer phase-coupling of gamma oscillations. Selective NMDA receptor antagonism, selective NR2B subunit-containing receptor antagonism and reduced *D*-serine levels caused a similar selective deceleration of HFγ, whereas increasing NMDA receptor activation through exogenous NMDA, *D*-serine or mGluR group 1 agonism selectively accelerated HFγ.

The NMDA-receptor hypofunction-induced phase-coupling of the normally independent gamma-generating networks is likely to cause abnormal cross-layer interactions, which may

distort perceptions due to aberrant matching of top-down information with bottom-up information. If decelerated HFγ and subsequent cross-layer synchronisation also underlies pathological psychosis, acceleration of HFγ could be the target for improved antipsychotic therapy.

Keywords

Gamma oscillation, ketamine, phencyclidine, NMDA receptor, hallucinogenic, psychotomimetic

Introduction

Hallucinations are perceptions in the absence of a stimulus. Where hallucinations are often auditory in schizophrenia, hallucinations associated with neurodegenerative dementias like Lewy body Dementia, and Parkinson's disease with dementia are normally visual (Metzler-Baddeley 2007). Hallucinations, and distortions of visual perception (Muetzelfeldt et al. 2008) are also a desired action of dissociative drugs like the N-methyl-D-aspartic acid (NMDA) receptor antagonists ketamine and phencyclidine (PCP). Because a single sub-anaesthetic dose of ketamine or PCP is psychotomimetic (Farber 2003) and agents that enhance NMDA receptor function are antipsychotic (Kantrowitz et al. 2010; Schlumberger et al. 2010; Marek et al. 2010), NMDA receptor hypofunction is regarded a shared process in both psychotic pathologies and

substance abuse drugs (Coyle 2006). Understanding the mechanism by which NMDA receptor hypofunction causes aberrant perceptions may lead to better antipsychotic treatment.

Perceptions may arise from matching of data-driven (bottom-up) information processing in the sensory cortices with (top-down) information driven by previous experiences stored in higher cortical areas. This process requires neuronal synchronization with millisecond-precision provided by network oscillations at gamma frequencies (30-120 Hz) (Herrmann et al. 2004; Engel et al. 2001). Reduced NMDA receptor-mediated activation of interneurons in cortical networks leads to pyramidal neuron hyperexcitability (Homayoun and Moghaddam 2007), which was hypothesized to cause aberrant perceptions by disruption of gamma synchronization (Marek et al. 2010). However, psychosis and hallucinations have rather been associated with gamma hypersynchronization (Hakami et al. 2009; Spencer et al. 2009; Flynn et al. 2008; Spencer et al. 2009; Herrmann and Demiralp 2005).

In the neocortex high-frequency gamma oscillations (HFγ; > 70 Hz) coexist with low-frequency gamma oscillations (LFγ; < 70 Hz) and the two can operate independently and serve different aspects of information processing processing (Wyart and Tallon-Baudry 2008; Vidal et al. 2006) (Crone et al. 2006). Recently we demonstrated that HFγ and LFγ can coexist in the same column of the visual cortex *in vitro* and operate independently (Oke et al. 2010). Interestingly the NMDA receptor antagonist APV selectively reduced the dominant frequency of HFγ so that it approached the frequency of the unaltered LFγ (Oke et al. 2010).

We therefore propose that NMDA receptor hypofunction causes phase-coupling of two normally phase-independent gamma generating networks, causing hypersynchrony and a distortion of perception due to aberrant matching of top-down information with bottom-up information. Here we test the effect of NMDA receptor hypofunction on HFγ and LFγ recorded

in the rat visual cortex *in vitro* and demonstrate that NMDA receptor hypofunction phase-couples the two gamma generating networks.

Materials and methods

Preparation

Male adult Sprague Dawley rats (200-300 g, Charles-River, Margate, UK) were anaesthetized with by intraperitoneal injection of a ketamine (75 $mg.kg^{-1}$) / medetomidine (1 $mg.kg^{-1}$) mixture and killed by cardiac perfusion with a chilled sucrose-based solution containing 189 mM sucrose, 2.5 mM KCl, 26 mM $NaHCO_3$, 1.2 mM NaH_2PO_4, 0.1 mM $CaCl_2$, 5 mM $MgCl_2$, 10 mM *D*-glucose; pH 7.4. All procedures conformed to the UK Animals (Scientific Procedures) Act 1986. The brain was removed and coronal slices (400 μm thick) were cut around 7-6 mm caudal from bregma. The dorsal neocortex containing the visual cortex areas V1 and V2 was isolated from the rest of the slice by scalpel cuts in chilled sucrose-based solution. Slices were either immediately placed at the interface between artificial cerebrospinal fluid (aCSF, at 7 ml/min) and moist carbogen (95% O_2 and 5 % CO_2 at 300 ml/min) at 32 ºC, or stored in a static interface type chamber at 23 ºC for later use. aCSF contained 125 mM NaCl, 3 mM KCl, 26 mM $NaHCO_3$, 1.25 mM NaH_2PO_4, 2 mM $CaCl_2$, 1 mM $MgCl_2$, 10 mM *D*-glucose; pH was set at 7.4. Slices were allowed to recover for one hour before recordings started.

Electrophysiological recordings

Gamma oscillations were evoked by adding kainate (400 nM) and the muscarinic acetylcholine receptor agonist carbachol (20 μM) (Buhl et al. 1998; Oke et al. 2010), and left to develop for one hour before oscillation characteristics were further explored.

Field potentials were recorded with aCSF-filled glass pipette recording electrodes (4-5 MΩ), amplified with Neurolog NL104 AC-coupled amplifiers (Digitimer, Welwyn Garden City, UK), band-pass filtered at 1-200 Hz with Neurolog NL125 filters (Digitimer), and any noise locked to the mains supply (50 Hz) was removed with Humbug noise eliminators (Digitimer). The signal was then digitized and sampled at 2 kHz using a CED-1401 (Cambridge Electronic Design, Cambridge, UK) and Spike-2 software (Cambridge Electronic Design). Slices were scanned for sites where high-frequency gamma oscillations and low-frequency gamma oscillations were found in the same column, which was usually in the medial part of the secondary visual cortex.

Intracellular current-clamp recordings were made using sharp (60-80 MΩ) pipettes, filled with 3 M potassium methylsulphate. Using a MX1641 motorized microdrive (Siskyou, Grants Pass, OR, USA) the electrode was driven (at 5 μm steps) into the tissue parallel to the layers up to a depth of 250 μm in search for neurons. The membrane potential was amplified using an Axoclamp-2A amplifier (Axon Instruments, Burlingham, CA, USA), low-pass filtered at 2 kHz and sampled at 10 kHz. Impaled cells were first inspected and accepted for recording if the input resistance was greater than 30 MΩ, the resting membrane potential was stable and more polarized than -55 mV in the presence of kainate and carbachol, and action potentials were overshooting.

Drugs were applied at about two hours after application of kainate and carbachol when the oscillation power and frequency were stable. Drug-induced changes after 25 minutes were compared with baseline values. Drugs were used diluted from the following frozen stock solutions. Ketamine; 50 mM in H_2O, PCP; 2 mM in H_2O (5S,10R)-(+)-5-Methyl-10,11-dihydro-5H-dibenzo[a,d]cyclohepten-5,10-imine maleate (MK-801); 10 mM in H_2O, $ZnCl_2$; 30 μM in H_2O, (aR,bS)-a-(4-Hydroxyphenyl)-b-methyl-4-(phenylmethyl)-1 -piperidinepropanol maleate (Ro 25-6981); 10 mM in H_2O, (S)-3,5-Dihydroxyphenylglycine (DHPG); 10 mM in H_2O. D-serine was directly added to the aCSF. The *D*-serine metabolising enzyme *D*-amino acid oxidase (DAAO); 800 U/ml was derived from rhodotorula gracilis and kindly donated by Professor Dale (University of Warwick). Ketamine, Ro 25-6981 and MK-801 were purchased from Tocris (Bristol, UK). All other drugs and aCSF salts were purchased from Sigma (Poole, UK). Ketamine and PCP were washed out for 30 minutes and if the drug effect was reversible a second higher concentration of the same drug was applied.

Data analysis

The oscillation power was calculated from 60 s recording epochs by fast Fourier transforms (1 Hz bin size, Hanning window), using Spike-2 software. The gamma frequency band was set at 20-80 Hz for recording at 32 °C, taking into account the temperature dependence of gamma oscillations observed in the visual cortex (Oke et al. 2010). The dominant oscillation frequency was determined as the frequency of peak power in the power spectrum smoothed by a 5-point simple moving average. To take into account possible changes in dominant oscillation frequency

the power was averaged over -5 Hz to 5 Hz of the dominant frequency. Waveform cross-correlograms were calculated over 60 s digitally high-pass filtered (FIR at 10 Hz) epochs.

To obtain membrane waveform averages field potential recordings were band-pass filtered (with a phase-true FIR filter) from 10 to 200 Hz. The maximum amplitude for gamma cycles was determined for this signal so that on average one cycle per second exceeded this value. Gamma cycles of medium (0.4-0.6 times the maximum) amplitude were marked at their trough minimum and waveform averages of gamma cycles (> 300 cycles, time-zeroed at the sorted marks) were then calculated from the 10 Hz high-pass (FIR) filtered membrane potential.

To determine the relationship between different events peri-event interval distributions (between -50 ms and 50 ms) were calculated from the timings of the different events and a distribution deviating significantly from a uniform distribution was considered to indicate a relationship between the timing of the two events. To determine the phase relationship between oscillations in recordings from different layers, peri-event intervals were calculated using MATLAB software (The MathWorks, Natick, USA). Simultaneous 100 s recordings were band-pass filtered (with a phase-true FIR filter) at±5 Hz of the dominant frequency of LFγ (determined in layer V) and HFγ (determined in layer III). A Hilbert transform provided a discrete-time analytic signal that was converted to phase angles in radians. From the Hilbert-peak times from both recordings peri-event interval distributions were calculated.

Statistics

Data are expressed as means ± standard error of the mean (SEM), *n* indicates the number of slices or cells tested. The effect of drugs was tested by unpaired comparison with matched controls, using a two-tailed Student's *t*-test with and alpha level of 0.05. Deviation from a uniform distribution was determined with the Kolmogorov-Smirnov (K-S) Z test with and alpha level of 0.05.

Results

High-frequency gamma oscillations coexists with low-frequency gamma oscillations

We induced rhythmic field potential oscillations in cortex slices by bath application of kainate (400 nM) and carbachol (20 μM) that substitute for the glutamatergic and cholinergic inputs lost due to the slicing (Oke et al. 2010; Buhl et al. 1998). Oscillations had substantial power in the gamma frequency range (example in Figs. 1A*i*/B*i*), which was set at 20-80 Hz for recording at 32 °C, taking into account the temperature dependence of gamma oscillations (Oke et al. 2010). After one hour the visual cortex in each slice was scanned along layer IV to select a cortical column with oscillatory activity with power peaks in both the low-frequency gamma oscillation (LFγ) frequency band (20-45 Hz) and the high-frequency gamma oscillation (HFγ) frequency band (46-80 Hz) range (Oke et al. 2010), which was usually found in area V2M (Figure S1). Simultaneous field potential recordings were then made from layer III (0.5 mm from pial surface) and from layer V (1.2 mm from pial surface, Figure S1) of the selected column. The oscillatory activity in layer III (example in Figure 1A*i*, grey trace) was invariably faster than the

oscillatory activity in layer V (example in Figure 1A*i*). The power spectrum of the recording from layer III peaked at frequencies in the HFγ range (Table 1, example in Figure 1B*i*, grey line), whereas the power spectrum of the recording from layer V peaked at frequencies in the LFγ range (Table 1, example in Figure 1B*i*, black line).

Ketamine selectively decelerates HFγ

Application of the psychotomimetic drug ketamine (10 μM) reduced the dominant frequency of HFγ in layer III, without affecting the dominant frequency of LFγ in layer V (Table 1, example in Figure 1A*ii* and 1B*ii*). We determined the change in dominant frequency of HFγ in layer III and LFγ in layer V at 25 minutes after application of different ketamine concentrations and compared it with that after 25 minutes of continued perfusion with control aCSF (Table 1). Ketamine caused a significant reduction in dominant frequency of HFγ at concentrations of 1 μM and up (Figure 1C). The ketamine-induced deceleration of HFγ in layer III, defined as the ketamine-induced reduction in dominant frequency minus the change with control aCSF, as function of ketamine concentration. (Figure 1C, grey symbols) was fitted with a sigmoid function of the form: effect = maximum effect/(1 + ([drug]/EC_{50})$^{-h}$)), with a maximum effect of 22.1±0.7 Hz, a concentration of half maximum effect (EC_{50}) of 2.7±0.3 μM and a slope (*h*) of 1.1±0.1. This EC_{50} is well within the range of concentrations obtained with sub-anaesthetic doses used recreationally (shaded area in Figure 1C). The ketamine-induced deceleration of LFγ in layer V was only significant at very high concentrations (Figure 1C, black symbols). To allow for the frequency shift, the effect of ketamine on dominant gamma oscillation power was assessed by taking the average power over +5 Hz and -5 Hz from the dominant frequency. The

dominant HFγ power in layer III increased at lower concentrations and decreased at higher concentrations of ketamine (Figure 1D, grey symbols). The increase in dominant LFγ power in layer V at concentrations from 10 μM (Figure 1D, black symbols) may well reflect the contribution of decelerated HFγ in layer III. Effects of ketamine were completely reversible up to a concentration of 3 μM (not shown).

Deceleration of HFγ causes hypersynchrony

Under control conditions HFγ in layer III was independent of LFγ in layer V (Oke et al. 2010). In the presence of ketamine the difference between the dominant frequency of LFγ in layer V and that of the decelerated HFγ in layer III became so small that there was a possibility that the two gamma oscillation generating networks could become phase-locked. We tested the prediction that ketamine would increase the phase-link between the two oscillators, by determining the phase relationship between HFγ in layer III and LFγ in layer V from the peri-event intervals, calculated from a Hilbert transform of band-pass (± 5 Hz around dominant frequency) filtered recordings. Before ketamine, the peri-event interval distribution was not different from uniform in 6 out of 7 slices (K-S test $P< 0.05$, example in Figure 2A*i*), indicating the absence of a relationship between the phase of HFγ in layer III and the phase of LFγ in layer V. After ketamine (10 μM) the peaks in the inter-event distribution showed a significant relationship between the oscillation phase in layer III and that in layer V (example in Figure 2A*ii*). The K-S test Z increased from 1.11±0.11 in control to 4.23±0.21 in ketamine (Paired Student's t-test $P< 0.001$, $n= 7$, Figure 2A*iii*). On average layer III gamma troughs were 4.3±0.5 ms ahead of layer V gamma troughs. This indicates that, whereas in control the two oscillators

operate independently, the ketamine-induced deceleration of HFγ in layer III causes phase-coupling of the gamma generating networks in layer III and layer V.

Under control conditions LFγ in layer V is spatially coherent, unlike HFγ in layer III (Oke et al. 2010). To test whether the phase-coupling of the decelerated HFγ in layer III to LFγ would increase the spatial coherence of the gamma oscillation in layer III, we determined the cross correlation maximum between two electrodes placed 500 μm apart in layer III of the same slice. Cross correlation was small in control (example in Figure 2B*i*), but increased in the presence of ketamine (10 μM, example in Figure 2B*ii*). For five slices the cross correlation in layer III increased from 0.22±0.02 in control to 0.50±0.05 in ketamine (paired Student's *t*-test $P< 0.01$, Figure 2B*iii*). For the same slices the cross correlation maximum between two electrodes placed 500 μm apart in layer V was not affected by ketamine (0.54±0.05 in control versus 0.58±0.06 in ketamine, *n.s.*). This suggests that the increase in spatial coherence of gamma oscillations in layer III is due to the phase coupling of the decelerated HFγ in layer III to LFγ in layer V.

Ketamine causes entrainment of layer III pyramidal neurons by LFγ

Like other cortical gamma oscillations (Buhl et al. 1998; Cunningham et al. 2003), HFγ in layer III is dependent on recurrent inhibition (Oke et al. 2010) and layer III pyramidal neuron firing is entrained by rhythmic IPSCs and EPSCs phase-locked to HFγ in layer III (unpublished observations MV). To test whether ketamine affects the relationship between the activity of layer III pyramidal neurons and the gamma oscillations in the different layers, we recorded cells in layer III under sharp electrode current-clamp conditions. Six cells identified as pyramidal neurons (see Figure S2) were recorded before and after ketamine (10 μM).

To test the relationship between action potential firing times and gamma oscillation phase, neurons were made to fire at ~ 2 Hz by manually adjusting the holding current. The distribution of intervals between action potential peaks (500 per neuron) and HFγ troughs in layer III (example in Figure 3A*i*) was tested for uniformity. For 5 out of 6 neurons the spike timing distribution showed a significant relationship (K-S test for uniformity, $P< 0.05$) between firing and HFγ troughs in layer III, with the peak firing probability in these neurons 4.3±0.7 ms ahead of the HFγ trough. In contrast to the entrainment of firing by HFγ, the distribution of intervals between action potential peaks and LFγ troughs in layer V showed no entrainment of the same six layer III pyramidal neurons by LFγ in layer V (example in Figure 3B*i*).

In the presence of ketamine (10 μM) the firing of the same layer III pyramidal neurons was still entrained by the now decelerated HFγ in layer III, but the relation was less tight (example in Figure 3A*ii*). The K-S test *Z* was reduced from 2.96±0.26 in control to 2.47±0.31 in ketamine (paired Student's *t*-test $P< 0.05$, $n= 6$, Figure 3A*iii*). However, for 4 out of 6 layer III pyramidal neurons the firing was now entrained by LFγ in layer V (example in Figure 3B*ii*), with the peak firing probability in these neurons 0.5±1.0 ms after the HFγ trough. The K-S test *Z* increased from 0.95±0.14 in control to 1.87±0.19 in ketamine (paired Student's *t*-test $P< 0.01$, $n= 6$, Figure 3B*iii*). These observations demonstrate that layer III pyramidal neurons that under normal conditions ignore the LFγ in layer III, become entrained by it in the presence of ketamine.

Ketamine increases rhythmic synaptic inputs.

All pyramidal neurons recorded received a constant barrage of IPSPs and EPSP. To determine how synaptic inputs are related to the different gamma oscillations, we held the same neurons

manually just below firing threshold and constructed the membrane potential waveform averages, time-zeroed at the trough of medium-amplitude HFγ gamma cycles in layer III (example in Figure 3C*i*). The membrane potential gamma cycle had its peak amplitude 3.4±0.6 ms ahead of the HFγ trough in layer III. The waveform averages of the membrane potential time-zeroed to the LFγ troughs in layer V (example in Figure 3D*i*) show that the membrane oscillation was only weakly coupled to LFγ in layer V, peaking 1.3±0.8 ms ahead of the LFγ trough.

In the presence of ketamine the membrane potential waveform average time-zeroed at the decelerated HFγ troughs in layer III was larger (example in Figure 3C*ii*) and peaked later (1.0±0.7 ms, paired Student's *t*-test $P< 0.01$, $n= 6$,). The maximum (peak-to-trough) amplitude was 0.23±0.06 mV in ketamine versus 0.18±0.04 mV in control (paired Student's *t*-test $P< 0.05$, $n= 6$, Figure 3C*iii*). Ketamine strongly increased the maximum amplitude of the membrane potential waveform average for LFγ troughs in layer V (example in Figure 3D*ii*), without affecting the peak time (0.4±0.7 ms after the LFγ trough, *n.s.*). The maximum amplitude was 0.26±0.06 mV versus 0.10±0.03 mV in control (paired Student's *t*-test $P< 0.01$, $n= 6$, Figure 3D*iii*). These observations demonstrate that ketamine increases the LFγ-related rhythmic synaptic inputs to layer III pyramidal neurons.

PCP decelerates HFγ and causes hypersynchrony

The psychotomimetic drug PCP has a similar NMDA receptor-antagonistic action to ketamine and we predicted that PCP would have a ketamine-like effect on gamma oscillations in the visual cortex. Like with ketamine, application of 1 μM PCP reversibly decelerated HFγ in layer III, but did not affect the dominant frequency of LFγ in layer V (Table 1, example in Figure

S3A/B). Like ketamine, 1 μM PCP phase-locked the gamma-generating networks in layer III and layer V that were independent in control (Figure S3C). The deceleration of HFγ in layer III as function of PCP concentration (Figure S3D) was fitted with a sigmoid function with a maximum effect of 21.7±0.9 Hz, an EC_{50} of 0.16±0.02 μM and a slope of 1.7±0.3. PCP suppressed the dominant HFγ power at higher concentrations and increased the dominant LFγ power at intermediate concentrations (Figure S3E), possibly due to the contribution from the decelerated HFγ in layer III. At concentrations obtained with doses used to induce hallucinations PCP has the same network effects as ketamine.

NMDA receptor modulating drug effects

Ketamine and PCP are not selective NMDA receptor antagonists and may exert their effect through inhibition of I_h (Tanabe 2007) and/or dopamine D_2 receptor stimulation (Seeman et al. 2009). Therefore we tested the effect of the selective non-competitive NMDA receptor antagonist MK-801. MK-801 (10 μM) decelerated HFγ, but left the dominant frequency of LFγ unchanged (Table 1). MK-801 increased the dominant power of both HFγ and LFγ (Table 1). NMDA receptor activation also requires occupation of the glycine site by its endogenous ligand *D*-serine (Oliet and Mothet 2009). We reduced endogenous *D*-serine levels by increasing *D*-serine metabolism by applying the enzyme DAAO. DAAO (0.17 U/ml, 60 minutes) selectively decelerated HFγ (Table 1, example in Figure 4A). These observations, together with the increase in HFγ power observed with the competitive NMDA receptor antagonist APV (Oke et al. 2010), confirm that the HFγ-decelerating effect of ketamine and PCP is mediated through NMDA receptor antagonism.

In order to determine which NMDA receptor type is responsible we tested the effect of Ro 25-6981 (10 μM), a selective antagonist of NR2B subunit-containing NMDA receptors (Fischer et al. 1997) and of nanomolar zinc, which selectively blocks NR2A subunit-containing NMDA receptors (Paoletti et al. 1997). Ro 25-6981 selectively decelerated HFγ, increased dominant LFγ power and reduced dominant HFγ power (Table 1, example in Figure 4B). However, zinc (30 nM $ZnCl_2$) had no effect on the dominant frequency of HFγ or LFγ or on their dominant gamma power (Table 1). These observations indicate that the deceleration of HFγ by NMDA receptor antagonists is mediated by antagonism of NR2B subunit-containing NMDA receptors.

Based on the observation that NMDA receptor hypofunction can cause phase-coupling of the gamma oscillators by selectively decelerating HFγ, we predicted that the opposite effect would be obtained by increasing NMDA receptor activation. To test this we applied NMDA directly (Mann and Mody 2010) to slices with HFγ and LFγ. NMDA (3 μM) selectively accelerated HFγ and suppressed the gamma power of both HFγ and LFγ (Table 1). NMDA receptor activity depends on the activation of the glycine site of the receptor. Increasing glycine site occupation by applying a high concentration of *D*-serine (100 μM) selectively accelerated HFγ without affecting oscillation power (Table 1, example in Figure 4C). NMDA receptor activation can also be increased by activation of metabotropic glutamate group I receptors (Pisani et al. 1997). In line with this the metabotropic glutamate group I receptor agonist DHPG (10 μM) selectively accelerated HFγ, without affecting the oscillation power (Table 1, example in Figure 4D). These observations confirm that, whatever the method, increasing NMDA receptor activity selectively accelerates HFγ.

Discussion

We investigated the effect of psychotomimetic NMDA receptor antagonists ketamine and PCP and demonstrated that in the visual cortex NMDA receptor hypofunction causes phase-coupling of both HFγ in layer III and layer III pyramidal neuron activity to LFγ in layer V, by selectively decelerating HFγ. This effect is mediated through *D*-serine-dependent NR2B subunit-containing receptors, and can be reversed by increasing NMDA receptor activity.

Ketamine and PCP selectively decelerate HFγ in layer III with an EC_{50} within the sub-anaesthetic concentration range. At sub-anaesthetic doses ketamine strongly increases cortical LFγ power in the behaving rat (Hakami et al. 2009) and in healthy humans (Hong et al. 2010). This increase can be explained by the increase in HFγ power in layer III, and by the deceleration and increased spatial coherence of HFγ. Reducing the NMDA receptor-mediated drive of cortical interneurons increases pyramidal neuron firing rate (Homayoun and Moghaddam 2007) which, according to computational modelling, would increase in cortical gamma power (Spencer 2009). Because the spatial coherence of HFγ is relatively low in control conditions (Oke et al. 2010), recordings taken from the cortical surface are likely to miss the HFγ that can be recorded with indwelling electrodes and magnetoencephalography (Tallon-Baudry 2003). The deceleration of HFγ and subsequent phase-coupling to the spatially more-coherent LFγ will increase the spatial coherence of HFγ and the rhythmic IPSC amplitude in layer III pyramidal neurons, and hence will increase the power of the oscillation recorded with surface electrodes (illustrated in Figure 5).

Why does NMDA receptor modulation selectively affect HFγ frequency? The relatively high frequency of HFγ could be caused by 1) faster IPSC decay kinetics (Whittington et al. 1995; Heistek et al. 2010), 2) smaller IPSC amplitude (Atallah and Scanziani 2009), but see (Oke et al. 2010), 3) increased interneuron firing rate due to increased NMDA receptor-mediated depolarization and/or reduced tonic $GABA_A$ergic inhibition of interneurons (Mann and Mody 2010), or 4) the selective NMDA receptor-mediated activation of fast-firing parvalbumin-expressing interneurons (Middleton et al. 2008). The consistent, bi-directional effects of modulating NMDA receptor activation on HFγ frequency suggest that NMDA receptor hypofunction decelerates HFγ by reduced activation of fast-firing, probably parvalbumin-expressing interneurons in the superficial layers that drive HFγ. Interneurons involved in LFγ in layer V may not be dependent on NMDA receptor-mediated activation. Indeed, $GABA_A$ergic IPSCs in layer V neurons are NMDA receptor activation-independent (Ling and Benardo 1995). Because NMDA receptor-mediated modulation of interneuron activity can be presynaptic, NMDA receptor antagonists may selectively reduce glutamate release to interneurons involved in HFγ. Indeed, NR2B-containing (and not NR2A-containing) NMDA auto-receptors modulate glutamate release in visual cortex and are located in layer II/III (Li et al. 2009). This is consistent with the differential effects of zinc and Ro 25-6981 in decelerating HFγ.

Psychosis and hallucinations have been associated with increased cortical LFγ (Flynn et al. 2008; Spencer et al. 2009; Becker et al. 2009) and the gestalt-induced gamma oscillation is decelerated in the visual cortex of schizophrenics (Spencer et al. 2004). Because NMDA receptor hypofunction is a common factor in the action of substance abuse drugs and schizophrenia-associated psychosis (Coyle 2006; Farber 2003), the latter could be due to an increased

propensity of a cortical network to hypersynchronize (Spencer et al. 2009), due to network changes that can decelerate HFγ.

Firstly, parvalbumin-expressing fast-firing interneurons may be functionally impaired. In the visual cortex of schizophrenics parvalbumin-immunoreactivity is selectively reduced (Hashimoto et al. 2008). GABA synthesis is reduced in parvalbumin-expressing cortical interneurons (Hashimoto et al. 2003), possibly due to reduced activity of TrkB receptors, that are normally predominantly expressed on parvalbumin-expressing interneurons (Lewis et al. 2005), but are reduced in schizophrenics (Hashimoto et al. 2005). Increased activation of the remaining TrkB receptors may therefore have antipsychotic potential.

Secondly, the NMDA receptor-dependent activation of interneurons may be reduced. Although the total cellular expression of NR2 proteins is not consistently altered in the cortex of schizophrenics, the trafficking of NR2B subunit-containing NMDA receptors to their pre-and postsynaptic locations is impaired (Kristiansen et al. 2010). In the chronic low-dose MK-801-treated rat model the parvalbumin-expressing interneurons have a reduced NMDA receptor expression (Xi et al. 2009). As increased activation of NR2B subunit-containing NMDA receptors accelerated HFγ, selective facilitation of these receptors may therefore have antipsychotic potential.

NMDA receptor activation requires co-activation of the glycine site by its endogenous ligand *D*-serine (Oliet and Mothet 2009). Schizophrenia has been associated with aberrant NMDA receptor *D*-serine/glycine site function (Labrie and Roder 2010) and increasing *D*-serine levels has an antipsychotic-like profile (Kantrowitz et al. 2010; Marek et al. 2010). Interestingly, in the rat visual cortex glycine site agonists facilitate glutamate release in layer III by acting on presynaptic NR2B subunit-containing NMDA auto-receptors (Li et al. 2008). The deceleration of

HFγ with reducing endogenous *D*-serine levels and the acceleration with exogenous *D*-serine confirm that the deceleration of HFγ is involved in the psychotic action of NMDA receptor hypofunction.

NMDA receptor activation is facilitated by metabotropic glutamate receptor group 1 activation (Pisani et al. 1997) through mGluR5 receptors. Although the mGluR5 expression is not altered in the cortex of schizophrenics (Gupta et al. 2005), increasing mGluR5 receptor activity has promising antipsychotic effects (Schlumberger et al. 2010), possibly due to the acceleration of HFγ observed with DHPG.

Thirdly, non-NMDA receptor-dependent activation of fast-spiking interneurons may be impaired. Metabotropic glutamate receptor GluR2-selective agonists selectively activate fast-spiking interneurons in the cortex (Sun et al. 2009) and have an antipsychotic action (Marek et al. 2010). The expression of kainate receptor subunit GluR5 (not mGluR6) mRNA was reduced in cortical interneurons of schizophrenics (Woo et al. 2007). Because the GluR5 subunit-selective kainate receptor agonist ATPA accelerated HFγ frequency (Oke et al. 2010), selective GluR5 potentiators may have an antipsychotic potential (Marek et al. 2010).

At a cellular level the ketamine-induced deceleration of HFγ caused the firing of layer III pyramidal neurons to be entrained by LFγ in layer V. Whereas in control conditions the firing of pyramidal neurons in the superficial layers is independent of that in the deep layers, NMDA receptor hypofunction aligns the firing of the two populations, increasing the interactions between the layers (illustrated in Figure 5). Because the decelerated HFγ in layer III phase leads LFγ in layer V, as in the somatosensory cortex under control conditions (Buhl et al. 1998), the EPSPs from layer III pyramidal neurons may arrive just before the IPSCs in layer V pyramidal

neurons. This is likely to increase the information transfer between the layers during gamma oscillations. In addition it may increase the synaptic strength of layer III to layer V pyramidal neuron connections through Hebbian plasticity and change information transfer long-term. In addition the phase-coupling of neuronal firing across layers is likely to increase burst firing in layer V pyramidal neurons that stretch through all layers (Larkum et al. 1999; Larkum et al. 2004).

Functionally it is tempting to speculate how hallucinations can arise from the increased coupling of processes in the superficial layers and the deep layers. Co-existence of HFγ and LFγ is found throughout the cortex, including the auditory cortex and prefrontal cortex (Crone et al. 2006). In the visual cortex HFγ and LFγ are associated with different aspects of visual information processing (Wyart and Tallon-Baudry 2008; Vidal et al. 2006; Chaumon et al. 2009) and relate to the degree of top-down or bottom-up processing (Tallon-Baudry, personal communication). Conscious perception of complex visual stimuli may need the matching of stimulus-driven bottom-up information with memory-based top-down predictions (Wyart and Tallon-Baudry 2008; Herrmann et al. 2004; Engel et al. 2001). Top-down processes may modulate the temporal structure of bottom-up processes (Engel et al. 2001), and/or boost the response of layer V neurons when bottom-up and top-down information arrives simultaneously at basal and apical dendrites respectively (Siegel and Konig 2003; Larkum et al. 2004). The phase-coupling induced by NMDA receptor hypofunction may therefore cause erroneous matching and hence distortion of perception of bottom-up information, or even perception without it during hallucinations. *In vivo* experiments are needed to test the relationship between increased phase-coupling of HFγ and LFγ and psychosis.

The negative symptoms in schizophrenics are associated with gamma band hyposynchronisation (Spencer et al. 2009; Herrmann and Demiralp 2005), which poses the question how gamma band hypersynchronisation can arise from the same distorted network? Computational modelling has demonstrated that different kinds of network abnormalities associated with schizophrenia can produce gamma oscillation deficits as well as increases (Spencer 2009). We propose that even in a network with reduced LFγ, the coincidence of several of the modulatory factors that each can cause selective deceleration of HFγ in the superficial layers, may cause a temporary cross-layer gamma band hypersynchronization and consequent distortion of perception, due to aberrant matching of top-down information with bottom-up information. Our study suggests that a combination of therapies to counteract several of these modulating factors may provide the most effective antipsychotic therapy.

Disclosure/Conflict of Interest

The authors declare that, except for income received from the primary employer, or stipends unrelated to pharmaceutical corporations, no financial support or compensation has been received from any individual or corporation over the last three years of research and there are no personal financial holdings that could be perceived as constituting a potential conflict of interest.

Acknowledgments

We thank the Medical Research Council (UK) for support. We thank Professor Jefferys (University of Birmingham) for discussion and use of equipment. We thank B. Shakila and Professor Dale (University of Warwick) for the production and kind donation of DOOA.

Reference List

Atallah BV, Scanziani M (2009). Instantaneous modulation of gamma oscillation frequency by balancing excitation with inhibition. *Neuron* **62**: 566-577.

Becker C, Gramann K, Muller HJ, Elliott MA (2009). Electrophysiological correlates of flicker-induced color hallucinations. *Conscious Cogn* **18**: 266-276.

Buhl EH, Tamas G, Fisahn A (1998). Cholinergic activation and tonic excitation induce persistent gamma oscillations in mouse somatosensory cortex *in vitro*. *J Physiol (Lond)* **513**: 117-126.

Chaumon M, Schwartz D, Tallon-Baudry C (2009). Unconscious learning versus visual perception: Dissociable roles for gamma oscillations revealed in MEG. *J Cogn Neurosci* **21**: 2287-2299.

Coyle JT (2006). Substance use disorders and Schizophrenia: a question of shared glutamatergic mechanisms. *Neurotox Res* **10**: 221-233.

Crone NE, Sinai A, Korzeniewska A (2006). High-frequency gamma oscillations and human brain mapping with electrocorticography. *Prog Brain Res* **159**: 275-295.

Cunningham MO, Davies CH, Buhl EH, Kopell N, Whittington MA (2003). Gamma oscillations induced by kainate receptor activation in the entorhinal cortex *in vitro*. *J Neurosci* **23**: 9761-9769.

Engel AK, Fries P, Singer W (2001). Dynamic predictions: oscillations and synchrony in top-down processing. *Nat Rev Neurosci* **2**: 704-716.

Farber NB (2003). The NMDA receptor hypofunction model of psychosis. *Ann N Y Acad Sci* **1003**: 119-130.

Fischer G, Mutel V, Trube G, Malherbe P, Kew JN, Mohacsi E*, et al.* (1997). Ro 25-6981, a highly potent and selective blocker of N-methyl-D-aspartate receptors containing the NR2B subunit. Characterization in vitro. *J Pharmacol Exp Ther* **283**: 1285-1292.

Flynn G, Alexander D, Harris A, Whitford T, Wong W, Galletly C*, et al.* (2008). Increased absolute magnitude of gamma synchrony in first-episode psychosis. *Schizophr Res* **105**: 262-271.

Gupta DS, McCullumsmith RE, Beneyto M, Haroutunian V, Davis KL, Meador-Woodruff JH (2005). Metabotropic glutamate receptor protein expression in the prefrontal cortex and striatum in schizophrenia. *Synapse* **57**: 123-131.

Hakami T, Jones NC, Tolmacheva EA, Gaudias J, Chaumont J, Salzberg M*, et al.* (2009). NMDA receptor hypofunction leads to generalized and persistent aberrant gamma oscillations independent of hyperlocomotion and the state of consciousness. *PLoS One* **4**: e6755.

Hashimoto T, Bazmi HH, Mirnics K, Wu Q, Sampson AR, Lewis DA (2008). Conserved regional patterns of GABA-related transcript expression in the neocortex of subjects with schizophrenia. *Am J Psychiatry* **165**: 479-489.

Hashimoto T, Bergen SE, Nguyen QL, Xu B, Monteggia LM, Pierri JN*, et al.* (2005). Relationship of brain-derived neurotrophic factor and its receptor TrkB to altered inhibitory prefrontal circuitry in schizophrenia. *J Neurosci* **25**: 372-383.

Hashimoto T, Volk DW, Eggan SM, Mirnics K, Pierri JN, Sun Z*, et al.* (2003). Gene expression deficits in a subclass of GABA neurons in the prefrontal cortex of subjects with schizophrenia. *J Neurosci* **23**: 6315-6326.

Heistek TS, Timmerman AJ, Spijker S, Brussaard AB, Mansvelder HD (2010). GABAergic synapse properties may explain genetic variation in hippocampal network oscillations in mice. *Frontiers in Cellular Neuroscience* **4**: 18-doi:10.3389/fncel.2010.00018.

Herrmann CS, Demiralp T (2005). Human EEG gamma oscillations in neuropsychiatric disorders. *Clin Neurophysiol* **116**: 2719-2733.

Herrmann CS, Munk MH, Engel AK (2004). Cognitive functions of gamma-band activity: memory match and utilization. *Trends Cogn Sci* **8**: 347-355.

Homayoun H, Moghaddam B (2007). NMDA receptor hypofunction produces opposite effects on prefrontal cortex interneurons and pyramidal neurons. *J Neurosci* **27**: 11496-11500.

Hong LE, Summerfelt A, Buchanan RW, O'Donnell P, Thaker GK, Weiler MA*, et al.* (2010). Gamma and delta neural oscillations and association with clinical symptoms under subanesthetic ketamine. *Neuropsychopharmacology* **35**: 632-640.

Kantrowitz JT, Malhotra AK, Cornblatt B, Silipo G, Balla A, Suckow RF*, et al.* (2010). High dose D-serine in the treatment of schizophrenia. *Schizophr Res*: doi:10.1016/j.schres.2010.05.012.

Kristiansen LV, Bakir B, Haroutunian V, Meador-Woodruff JH (2010). Expression of the NR2B-NMDA receptor trafficking complex in prefrontal cortex from a group of elderly patients with schizophrenia. *Schizophr Res* **119**: 198-209.

Labrie V, Roder JC (2010). The involvement of the NMDA receptor D-serine/glycine site in the pathophysiology and treatment of schizophrenia. *Neurosci Biobehav Rev* **34**: 351-372.

Larkum ME, Senn W, Luscher HR (2004). Top-down dendritic input increases the gain of layer 5 pyramidal neurons. *Cereb Cortex* **14**: 1059-1070.

Larkum ME, Zhu JJ, Sakmann B (1999). A new cellular mechanism for coupling inputs arriving at different cortical layers. *Nature* **398**: 338-341.

Lewis DA, Hashimoto T, Volk DW (2005). Cortical inhibitory neurons and schizophrenia. *Nat Rev Neurosci* **6**: 312-324.

Li YH, Han TZ, Meng K (2008). Tonic facilitation of glutamate release by glycine binding sites on presynaptic NR2B-containing NMDA autoreceptors in the rat visual cortex. *Neurosci Lett* **432**: 212-216.

Li YH, Wang J, Zhang G (2009). Presynaptic NR2B-containing NMDA autoreceptors mediate gluta-matergic synaptic transmission in the rat visual cortex. *Curr Neurovasc Res* **6**: 104-109.

Ling DS, Benardo LS (1995). Recruitment of GABAA inhibition in rat neocortex is limited and not NMDA dependent. *J Neurophysiol* **74**: 2329-2335.

Mann EO, Mody I (2010). Control of hippocampal gamma oscillation frequency by tonic inhibition and excitation of interneurons. *Nat Neurosci* **13**: 205-212.

Marek GJ, Behl B, Bespalov AY, Gross G, Lee Y, Schoemaker H (2010). Glutamatergic (N-methyl-D-aspartate receptor) hypofrontality in schizophrenia: too little juice or a miswired brain? *Mol Pharmacol* **77**: 317-326.

Metzler-Baddeley C (2007). A review of cognitive impairments in dementia with Lewy bodies relative to Alzheimer's disease and Parkinson's disease with dementia. *Cortex* **43**: 583-600.

Middleton S, Jalics J, Kispersky T, LeBeau FE, Roopun AK, Kopell NJ*, et al.* (2008). NMDA receptor-dependent switching between different gamma rhythm-generating microcircuits in entorhinal cortex. *Proc Natl Acad Sci U S A* **105**: 18572-18577.

Muetzelfeldt L, Kamboj SK, Rees H, Taylor J, Morgan CJ, Curran HV (2008). Journey through the K-hole: phenomenological aspects of ketamine use. *Drug Alcohol Depend* **95**: 219-229.

Oke OO, Magony A, Anver H, Ward PD, Jiruska P, Jefferys JGR*, et al.* (2010). High-frequency gamma oscillations coexist with low-frequency gamma oscillations in the rat visual cortex *in vitro*. *Eur J Neurosci* **31**: 1435-1445.

Oliet SH, Mothet JP (2009). Regulation of N-methyl-D-aspartate receptors by astrocytic D-serine. *Neuroscience* **158**: 275-283.

Paoletti P, Ascher P, Neyton J (1997). High-affinity zinc inhibition of NMDA NR1-NR2A receptors. *J Neurosci* **17**: 5711-5725.

Pisani A, Calabresi P, Centonze D, Bernardi G (1997). Enhancement of NMDA responses by group I metabotropic glutamate receptor activation in striatal neurones. *Br J Pharmacol* **120**: 1007-1014.

Schlumberger C, Pietraszek M, Gravius A, Danysz W (2010). Effects of a positive allosteric modulator of mGluR5 ADX47273 on conditioned avoidance response and PCP-induced hyperlocomotion in the rat as models for schizophrenia. *Pharmacol Biochem Behav* **95**: 23-30.

Seeman P, Guan HC, Hirbec H (2009). Dopamine D2High receptors stimulated by phencyclidines, lysergic acid diethylamide, salvinorin A, and modafinil. *Synapse* **63**: 698-704.

Siegel M, Konig P (2003). A functional gamma-band defined by stimulus-dependent synchronization in area 18 of awake behaving cats. *J Neurosci* **23**: 4251-4260.

Spencer KM (2009). The functional consequences of cortical circuit abnormalities on gamma oscillations in schizophrenia: insights from computational modeling. *Front Hum Neurosci* **3**: 33.

Spencer KM, Nestor PG, Perlmutter R, Niznikiewicz MA, Klump MC, Frumin M*, et al.* (2004). Neural synchrony indexes disordered perception and cognition in schizophrenia. *Proc Natl Acad Sci U S A* **101**: 17288-17293.

Spencer KM, Niznikiewicz MA, Nestor PG, Shenton ME, McCarley RW (2009). Left auditory cortex gamma synchronization and auditory hallucination symptoms in schizophrenia. *BMC Neurosci* **10:85**: doi:10.1186/1471-2202-10-85.

Sun QQ, Zhang Z, Jiao Y, Zhang C, Szabo G, Erdelyi F (2009). Differential metabotropic glutamate receptor expression and modulation in two neocortical inhibitory networks. *J Neurophysiol* **101**: 2679-2692.

Tallon-Baudry C (2003). Oscillatory synchrony and human visual cognition. *J Physiol (Paris)* **97**: 355-363.

Tanabe M (2007). Inhibition of hyperpolarization-activated cation currents by phencyclidine and some sigma ligands in rat hippocampal CA1 pyramidal neurons in vitro. *Neuropharmacology* **53**: 406-414.

Vidal JR, Chaumon M, O'Regan JK, Tallon-Baudry C (2006). Visual grouping and the focusing of attention induce gamma-band oscillations at different frequencies in human magnetoencephalogram signals. *J Cogn Neurosci* **18**: 1850-1862.

Whittington MA, Traub RD, Jefferys JGR (1995). Synchronized oscillations in interneuron networks driven by metabotropic glutamate receptor activation. *Nature* **373**: 612-615.

Woo TU, Shrestha K, Amstrong C, Minns MM, Walsh JP, Benes FM (2007). Differential alterations of kainate receptor subunits in inhibitory interneurons in the anterior cingulate cortex in schizophrenia and bipolar disorder. *Schizophr Res* **96**: 46-61.

Wyart V, Tallon-Baudry C (2008). Neural dissociation between visual awareness and spatial attention. *J Neurosci* **28**: 2667-2679.

Xi D, Zhang W, Wang HX, Stradtman GG, Gao WJ (2009). Dizocilpine (MK-801) induces distinct changes of N-methyl-D-aspartic acid receptor subunits in parvalbumin-containing interneurons in young adult rat prefrontal cortex. *Int J Neuropsychopharmacol* **12**: 1395-1408.

Table 1 Pharmacological modulation of HFγ and LFγ

		LFγ in layer V			HFγ in layer III		
			power	frequency		power	frequency
Control values		***n***	**(μV²)**	**(Hz)**	***n***	**(μV²)**	**(Hz)**
		55	26±3	34.3±0.4	55	33±4	54.1±0.6
Changes		***n***	**(%)**	**Δ (Hz)**	***n***	**(%)**	**Δ (Hz)**
Control		8	101±6	-0.5±0.7	8	95±6	-0.7±1.0
Ketamine	10 μM	7	131±29	-2.0±0.8	7	112±19	-18.8±3.2 **
PCP	1 μM	6	99±25	-1.9±0.9	6	61±12 *	-22.2±2.8 **
MK-801	10 μM	5	163±21 *	-1.4±0.6	5	127±13*	-18.2±2.6 **
DAAO	0.17 U/ml	6	112±6	0.4±0.8	6	71±8 *	-10.4±1.4 **
Ro 25-6981	10 μM	4	161±18 **	-0.8±0.5	4	64±9 **	-20.1±2.2 **
$ZnCl_2$	30 nM	5	106±3	-1.1±1.2	5	114±6	-3.1±1.2
NMDA	3 μM	5	83±6 *	0.6±1.0	5	73±7 *	4.2±0.6 **
DHPG	10 μM	4	81±13	1.1±0.8	4	129±14*	5.7±1.6 **
D-serine	100 μM	5	93±8	-0.3±0.7	5	112±7	3.7±0.7 **

Recordings were made from layer III and layer V of slices with LFγ and HFγ. The drug-induced change of dominant gamma power (average over -5 Hz to +5 Hz of the dominant frequency, expressed as % of pre-drug power), and the drug-induced shift in dominant frequency (in Hz) of LFγ in layer V and HFγ in layer III is given as mean ± SEM for *n* slices. Drug effects are compared with the change after 25 minutes in control solution. Statistical significant differences (unpaired Student's *t*-test) are indicated as * for $P< 0.05$ and as **for $P< 0.01$.

Titles and legends to the figures

Figure 1. Ketamine decelerates selectively HFγ. **A.** Example of oscillatory activity simultaneously recorded in layer III (grey line) and layer V (black line) of a cortical column in area V2M, before (***i***) and 20 minutes after bath application of 10 μM ketamine (***ii***). Scale bars: 50 ms and 50 μV. **B.** Power spectrum of one-minute recordings from layer III and layer V of the slice in (A), before (***i***) and after ketamine (***ii***). Ketamine reduces the frequency of HFγ in layer III, without affecting LFγ in layer V. **C.** Concentration-effect relationship of the deceleration of the dominant oscillation frequency for HFγ in layer III (grey symbols) and LFγ in layer V (black symbols). Data are average and SEM. of 3-8 observations per concentration. For each concentration the ketamine-induced change in dominant frequency was compared with the change in control solution, with * indicating Student's *t*-test $P< 0.05$; **, $P< 0.01$ and *, $P< 0.001$. The deceleration as function of ketamine concentration is fitted with a sigmoid function for HFγ and with a smooth function for LFγ. Shaded area indicates concentrations reached with psycho-toxic ketamine doses in humans. **D.** Dominant gamma power (average from -5 Hz to + 5Hz from the dominant gamma oscillation frequency) normalized to control values as function of ketamine concentration for the same experiments as in (C). Details as in C. Data are fitted with smooth functions.

Figure 2. Ketamine increases phase-coupling. **A.** Peri-event interval distribution of the interval between phase peaks of the Hilbert-transform of HFγ in layer III and those of LFγ in layer V, before (***i***) and after 10 μM ketamine (***ii***) for the same slice as in Figure 1A/B. ***iii.*** *Z* value of the Kolmogorov-Smirnov test for uniform distribution for control and ketamine. Data are

mean ± SEM for *n*=7. Ketamine phase-locks the oscillation in layer III to the oscillation in layer V. Ketamine phase-locks the oscillation in layer III and the oscillation in layer V. **B.** Simultaneous recordings from layer III at locations 500 μm apart (top panel) and waveform cross-correlogram (bottom panel), before (***i***) and after 10 μM ketamine (***ii***). ***iii.*** Cross correlation maximum in control and ketamine. Data are mean ± SEM for *n*=5. Ketamine increases maximum cross-correlation between layer III sites.

Figure 3. Ketamine effect on layer III pyramidal neurons. **A.** Peri-event interval distribution of action potential peak times relative to HFγ troughs in layer III, before (***i***) and after 10 μM ketamine (***ii***). ***iii.*** *Z* value of the Kolmogorov-Smirnov test for uniform distribution in control and ketamine. Data are mean ± SEM for *n*= 6. **B.** Same as in (A), but relative to LFγ troughs in layer V. **C.** Membrane potential (held just below firing threshold) waveform average phase-zeroed to the HFγ troughs in layer III, before (***i***) and after ketamine (***ii***). Scale bars: 20 μV, 20 ms. ***iii.*** Maximum peak-to-trough amplitude of the postsynaptic potential (PSP) waveform average in control and ketamine. Data give mean ± SEM for *n*= 6. **D.** Same as in (C), but phase-zeroed zeroed to the LFγ troughs in layer V. Ketamine entrains layer III pyramidal neurons to LFγ troughs in layer V and increases LFγ-related rhythmic synaptic inputs.

Figure 4. Effect of NMDA receptor modulation on HFγ. **A.** Power spectrum of a one-minute recording from layer III before (grey line) and after reducing endogenous *D*-serine levels with DAAO (0.17 U/ml, 60 minutes, black line). **B.** Effect of the NR2B subunit-containing receptor antagonist Ro 25-6981 (10 μM, 25 minutes). Details as in (A). **C.** Effect of application of *D*-

serine (100 μM). Details as in (A). **D.** Effect of facilitating NMDA receptor function by DHPG (10 μM). Details as in (A).

Figure 5. Illustration of the effect of hypersynchrony within and across layers. Recordings of gamma oscillations (modeled by sinusoids) from extracellular electrodes in two positions (500 μm apart, indicated in left panel) of layer III (grey traces) and layer V (bottom traces). In control (left hand traces) oscillations in layer III positions are not phase-locked within the layer or with the oscillation in layer V. After ketamine (right hand traces) the oscillation is phase-locked within and between the layers, increasing the signal picked up from the surface (top traces: summation of sinusoids). Dotted lines indicate times where potential firing times of layer III and layer V pyramidal neurons in position A would be nearly simultaneous, facilitating cross-layer interactions.

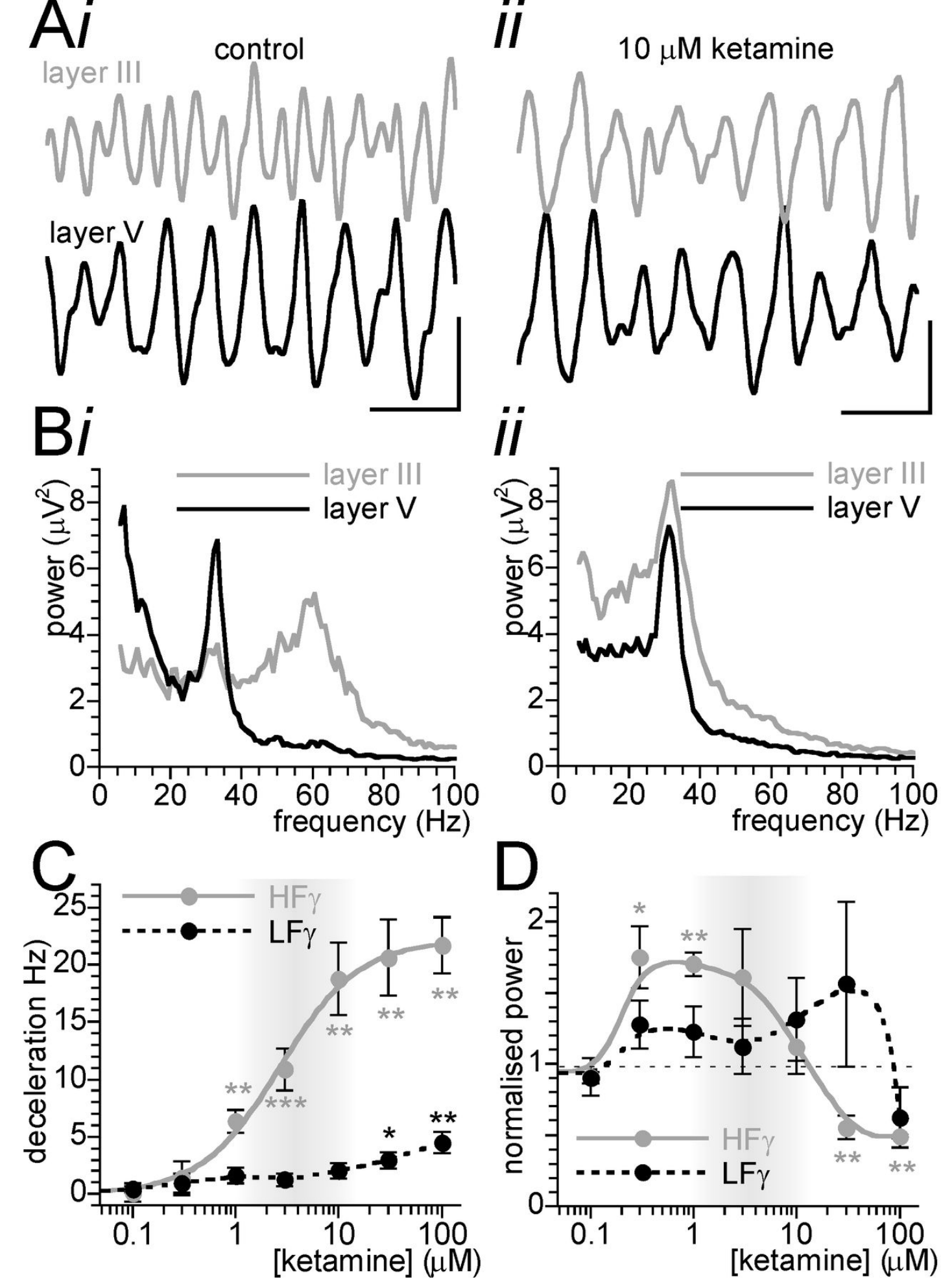
Ai
control
layer III
layer V
ii
10 μM ketamine
Bi
layer III
layer V
power (μV²)
frequency (Hz)
ii
layer III
layer V
power (μV²)
frequency (Hz)
C
HFγ
LFγ
deceleration Hz)
[ketamine] (μM)
D
normalised power
HFγ
LFγ
[ketamine] (μM)

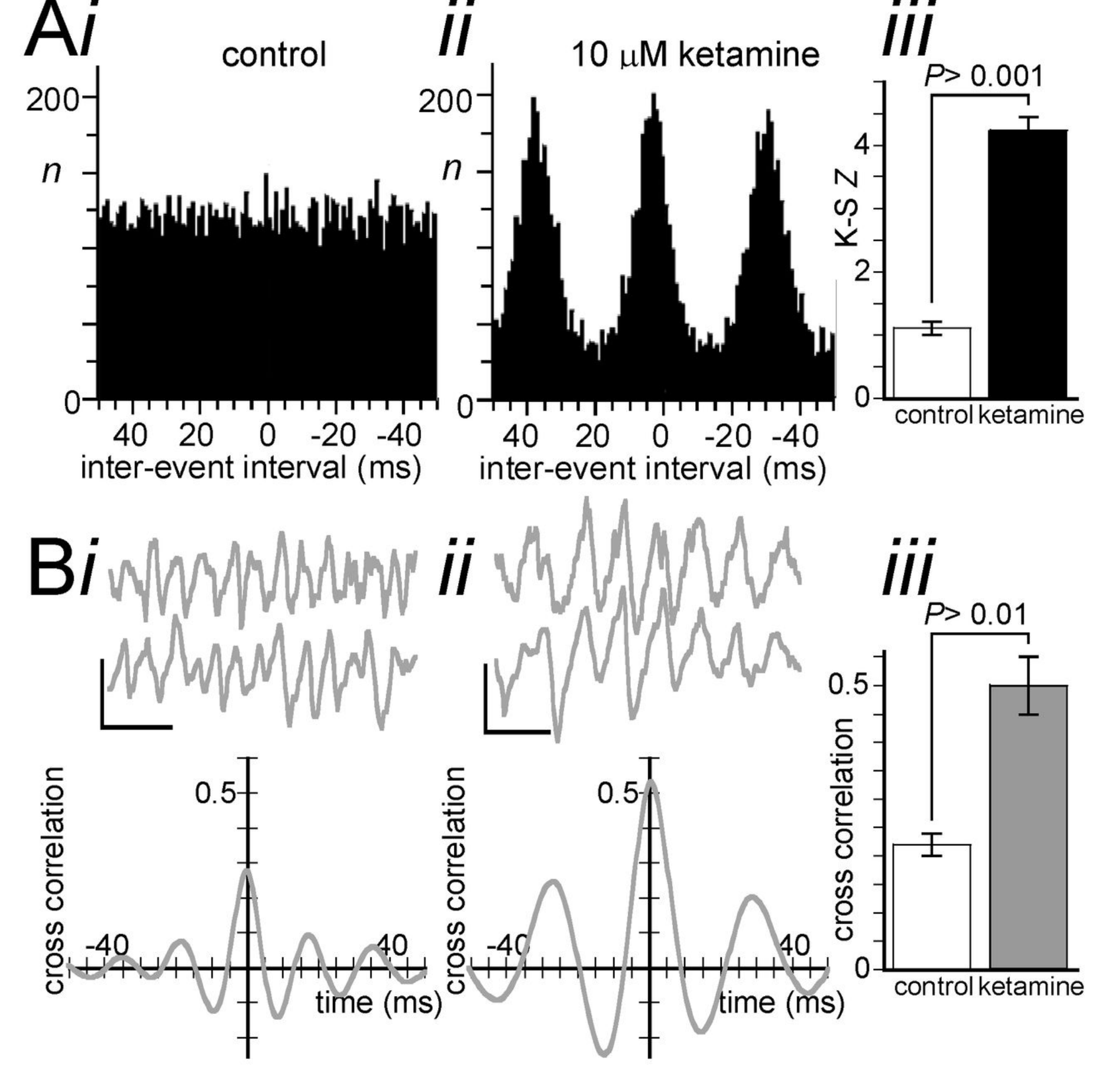
Ai
control
200
n
0
40 20 0 -20 -40
inter-event interval (ms)
ii
10 μM ketamine
200
n
0
40 20 0 -20 -40
inter-event interval (ms)
iii
P> 0.001
K-S Z
4
2
0
control ketamine
Bi
ii
iii
P> 0.01
0.5
cross correlation
-40
40
time (ms)
0.5
cross correlation
-40
40
time (ms)
0.5
cross correlation
0
control ketamine

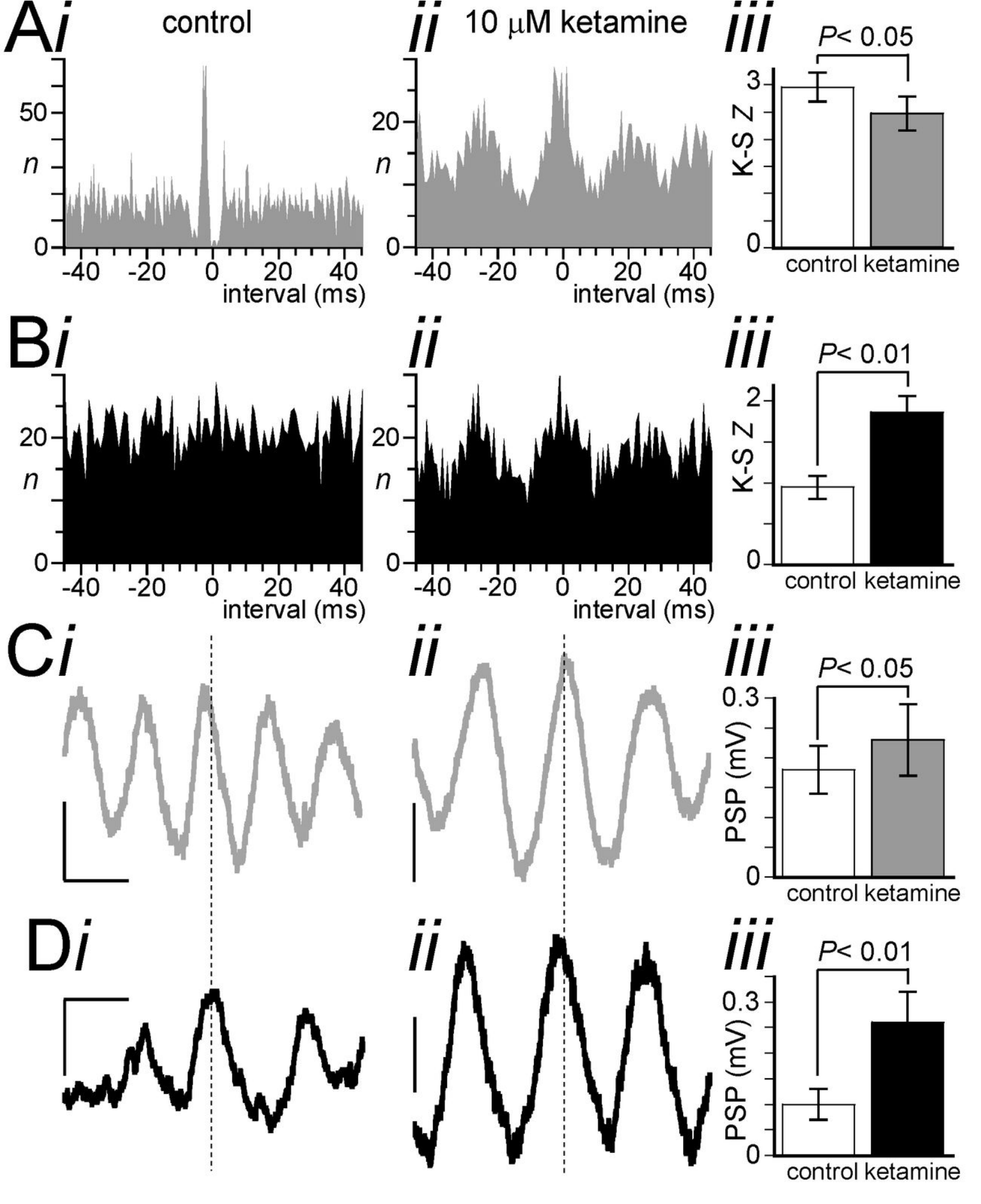
Ai
control
ii
10 μM ketamine
iii
P< 0.05
50
n
0
20
n
0
3
K-S Z
0
-40 -20 0 20 40
interval (ms)
-40 -20 0 20 40
interval (ms)
control ketamine
Bi
ii
iii
P< 0.01
20
n
0
20
n
0
2
K-S Z
0
-40 -20 0 20 40
interval (ms)
-40 -20 0 20 40
interval (ms)
control ketamine
Ci
ii
iii
P< 0.05
0.3
PSP (mV)
0
control ketamine
Di
ii
iii
P< 0.01
0.3
PSP (mV)
0
control ketamine

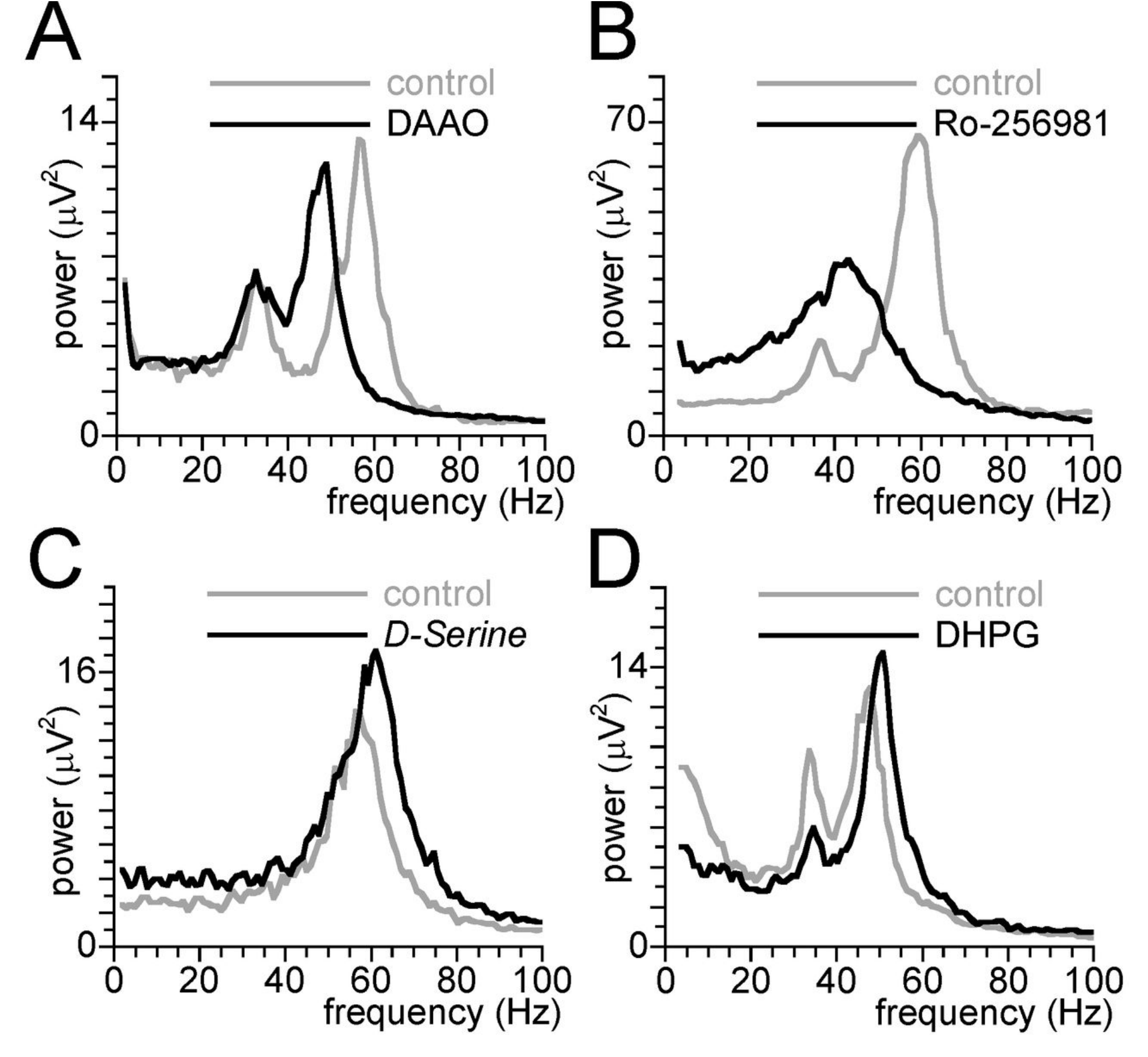
A
control
DAAO
14
0
power (μV²)
0
20
40
60
80
100
frequency (Hz)
B
control
Ro-256981
70
0
power (μV²)
0
20
40
60
80
100
frequency (Hz)
C
control
D-Serine
16
0
power (μV²)
0
20
40
60
80
100
frequency (Hz)
D
control
DHPG
14
0
power (μV²)
0
20
40
60
80
100
frequency (Hz)

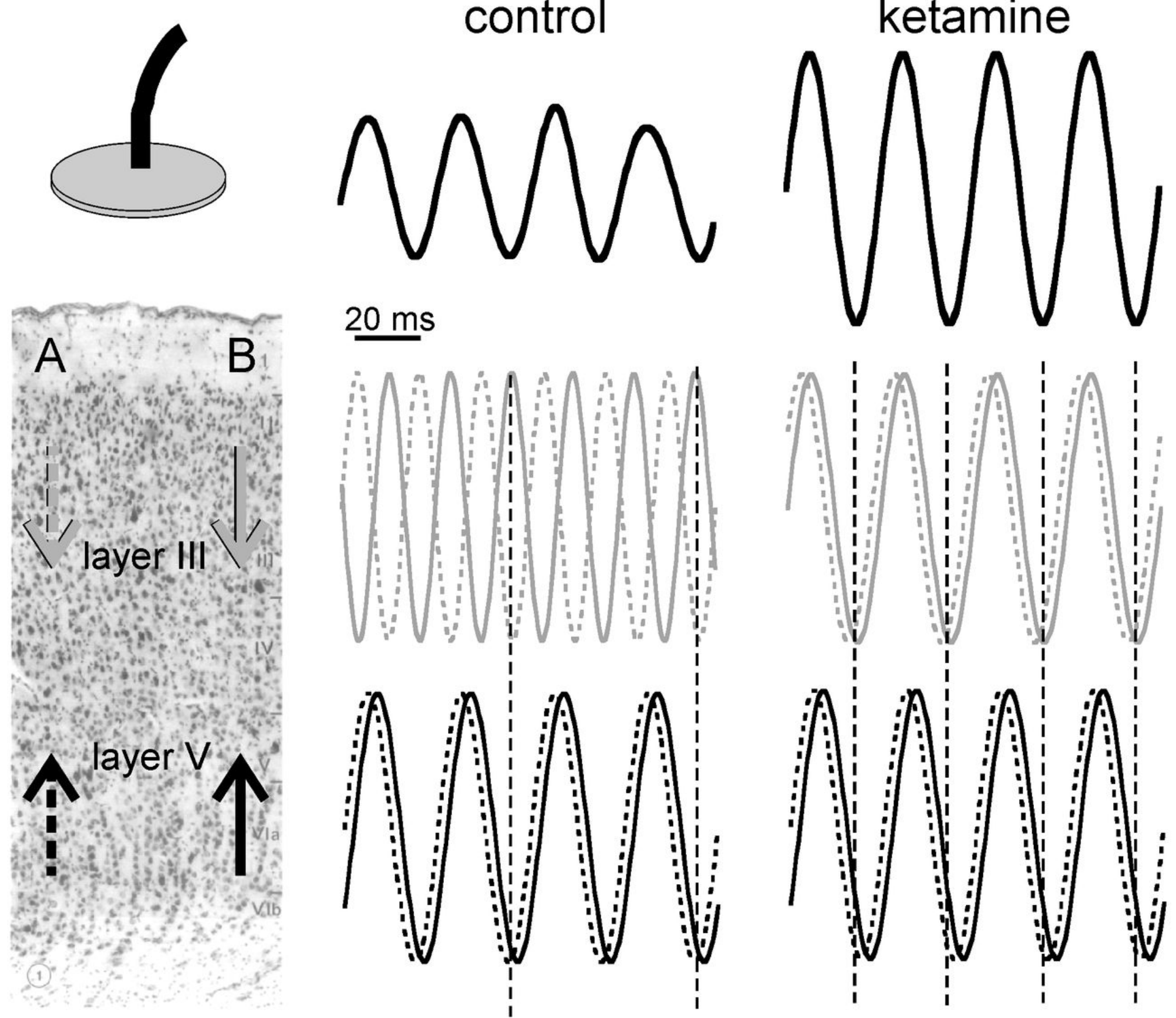
control
ketamine
20 ms
A
B
layer III
layer V
I
II
III
IV
V
VIa
VIb
1